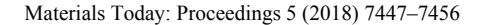


Available online at www.sciencedirect.com

ScienceDirect





www.materialstoday.com/proceedings

IMME17

Modelling and Microstructure of Friction Stir Welds of AA2014 Alloy: Different Tool Pin profiles

V. S. Gadakh, a*A. Kumar^b

^aAmrutvahini College of Engineering, Sangamner, Ahmednagar – 422 608, Maharashtra State, India.
^bNational Institute of Technology (NIT), Warangal – 506 004, Telengana State, India.

Abstract

In this work, the effect of different tool pin profiles such as triangle, square, pentagon and hexagon on friction stir welded butt joints of AA2014-T6 aluminium alloy using modelling and microstructure was investigated. Microstructure, mechanical properties and micro-hardness of all tool pin profiles are presented. The developed analytical heat generation models for different tool pin profiles are in good agreement with experimental results. From the developed models, sub-grain size at tool pin periphery using analytical modelling was almost corroborates with measured values. Smallest sub-grain size, high value of Zener-Holloman parameter and lowest peak temperature at tool pin periphery produced using square tool pin profile are the key mechanisms for improved friction stir welded joint properties.

© 2017 Elsevier Ltd. All rights reserved.

Selection and/or Peer-review under responsibility of International Conference on Emerging Trends in Materials and Manufacturing Engineering (IMME17).

Keywords: AA2014; friction stir welding; mechanical properties; microstructure; tool pin profile.

1. Introduction

Aluminium AA2014 is a heat treatable alloy; possesses good combinations of high strength (especially at elevated temperatures), toughness and is widely used in aircraft primary structure, heavy-duty forgings, plate, extrusions for aircraft fittings, wheels, major structural components, space booster tankage, truck frame and suspension components [1].

2214-7853 © 2017 Elsevier Ltd. All rights reserved.

Selection and/or Peer-review under responsibility of International Conference on Emerging Trends in Materials and Manufacturing Engineering (IMME17).

^{*} Corresponding author. Tel.: +91-2425-259015-272; fax: +91-2425-259016. E-mail address: vijay.gadakh@avcoe.org

Nomenclature

T_{max} Maximum temperature

 $\begin{array}{ll} H_{Probe} & Pin \ length, \ mm \\ R_{Probe} & Pin \ radius, \ mm \\ T_{solidus} & Solidus \ temperature \end{array}$

T* Temperature at tool pin periphery

 η Mechanical efficiency

 φ Heat generation due to plastic deformation

μ Friction coefficientF Vertical force, kN

τ_{contact} Contact shear stress, MPa Z Zener–Hollomon parameter Q Activation energy, kJ/mol

 ε Strain rate, s⁻¹

APR Tool advance per revolution

υ Weld Speed, mm/s

 ω Tool rotational speed, rev/s $Q_{\text{Eff/length}}$ Effective energy per weld length

Q_{Energy/length} Energy per weld length

β Transfer efficiency thk Workpiece thickness

R Universal gas constant, J/mol/K t time required for deformation, sec

d Sub-grain size, μm

However, this particular alloy is difficult to weld by fusion welding due to porosity formation, oxide inclusions, hot cracking, hydrogen pick-up during melting and re-solidification process, and dendrite structure formed in fusion welding which can affect the weld properties seriously [2]. In order to improve the joint efficiency as well as strength/mechanical properties newer techniques/method/processes must require initiative steps. Friction stir welding (FSW) is a solid-state joining process invented by The Welding Institute, UK in 1991 that is presently attracting considerable interest and has been extensively developed for alloys of Aluminium, Magnesium, Copper, Titanium, Steel as well as dissimilar materials[3].

The effect of tool pin geometry on mechanical properties and microstructure was already studied by past researchers using different tool pin profiles. The plastic deformation and the frictional heating of the workpiece are necessary for friction stirring and are influenced by the FSW tool design [4]. The shoulder and pin diameter; tool pin profile and pin length; and shoulder profile are important parameters in determining the quality of welds [5]. From the reported literature, it is understood that the tool pin geometry plays a crucial role for material flow, temperature history, grain size and mechanical properties in FSW process. Due to these aspects, a question arises why the results are varied for different tool pin geometry and thereby variation in mechanical properties and microstructures? With this consideration, in this paper, an attempt has been made to estimate and correlate the average grain size obtained from the analytical modelling for heat generation using different FSW tool pin profiles with microstructures. An attempt also has been made to correlate the isothermal contour plots obtained using Comsol Multiphysics with microstructures.

2. Experimental procedure

Two as-is received AA 2014-T6 aluminium alloy sheet of 300 mm×80 mm×5 mm thick were used to fabricate the joints. A non-consumable tool made of hot worked die steel hardened to ~53 HRC was used to fabricate joints. The FSW tool of 12 mm shoulder diameter, 6 mm pin diameter and pin length of 4.7 mm was employed for the experiments. The tools used for the present study are triangular (TR), square (SQ), pentagon (PEN), and hexagon

(IIEX) as shown in Fig. 1. The welding process is carried out on a vertical milling machine (Make: G. Dufour Montrenil, 7.5 hp, 1500 rpm). Experimental setup is shown in Fig. 2 (a-b). Before welding, the edges of the plates were face milled to get a smooth surface finish. The welding is performed in single pass, normal to the rolling direction on butt joint plate. Before temperature measurement preliminary experiments were carried out on bead-onplates by exploring the process parameters (Weld Speed, WS and tool rotational speed, TRS) based on the capabilities of the machine to the full extent using Taguchi's one parameter at one time approach. Then, by looking the surface morphologies of the FSWs and cutting the plate across the welds (to see if any defect), the working range of process parameters was decided. For pilot experimentation, TRS was varied from 710 – 1180 rpm and WS varied from 29 - 64 mm/min. It was observed that, at the lower TRS (710 rpm) and WS (29 mm/min) resulted in lack of stirring which leads to failure of joint due to low heat input [4]. The mechanical properties of the joints were evaluated and better properties were obtained at tool rotational speed of 900 rpm and weld speed of 49 mm/min. Now, the temperatures were recorded by keeping these parameters constant and varied the tool pin profile. Four trials for each experiment were conducted for temperature measurement to average of these values to minimize the pure experimental error. The depth of pin is kept constant (4.8 mm) throughout the experimentation. For temperature measurements, four 'K' type thermocouples (accuracy: ±1.5% of reading ±4°C for 400°C – 1000°C range and 1° resolution) of Ø 1.5 mm was used and the position of thermocouples are shown in Fig. 3

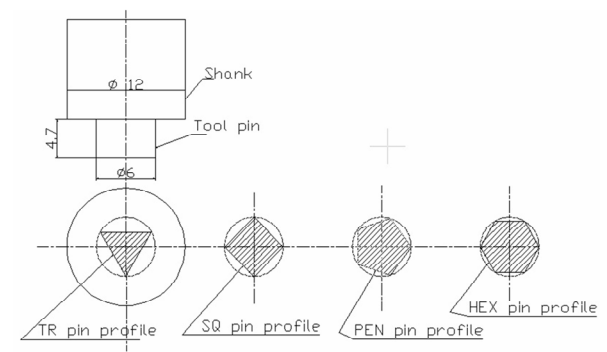


Fig. 1. A schematic diagram of FSW tool dimension and different tool pins used.





Fig. 2. (a) Close view of experimental setup, (b) Close view of four multimeters connected to thermocouples.

In order to determine the peak temperature at the weld zone (WZ), practically it is not possible because of severe plastic deformation due to high rotation of the tool. Hence the finite difference method was used to determine the peak temperature at the WZ. Comsol Multiphysics was used to understand the temperature isotherms across welds and estimate the maximum temperature (T_{max}) at WZ. After welding X- ray radiography was performed to detect any defects in the weldments. The microstructures at WZ of different FSWeldments were examined after preparation of sample using conventional metallographic technique and etching with Keller's reagent (2 ml HF, 3 ml HCL, 20 ml HNO₃, 175 ml H₂O). Microstructures at different locations of weldments were carried out using field emission gun-scanning electron microscope (FEG-SEM) (Make: JEOL; Model: JSM-7600F). The energy dispersive X-ray spectroscopy (EDS) equipped with SEM was used to analyze the chemical composition of the material.

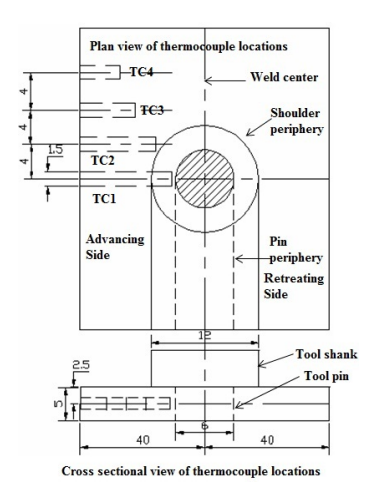


Fig. 3. A schematic diagram of thermocouple locations.

3. Development of empirical relationship between the ratio of temperature at tool pin periphery i.e. $(T^*/T_{solidus})$ and the effective energy level

The effective energy per weld length ($Q_{Eff/length}$) [6] is defined as the energy per weld length multiplied by the transfer efficiency (β , ratio of the pin length H_{Probe} to the work piece thickness, thk) and given as:

$$Q_{\text{Eff/length}} = \frac{H_{\text{probe}}}{\text{thk}} \cdot Q_{\text{Energy/Length}} = \beta \cdot Q_{\text{Energy/Length}}$$
(1)

In the current modelling, the empirical relationship between the ratio of temperature at tool pin periphery i.e. $(T^*/T_{solidus})$ and the effective energy level $(Q_{Eff/length})$ is developed based on pilot experimentation. The ratio of average temperature produced by each of the tool pin profile at tool pin periphery to the solidus temperature for AA 2014-T6 aluminium alloy was determined. From these values, the effective energy per weld length $(Q_{Eff/length})$ for different tool pin profiles was estimated as shown in Table 1. The empirical formula is given by

$$\frac{T^*}{T_{solidus}} = 1 \times 10^{-6} \times Q_{Eff}^2 - 0.0027 \times Q_{Eff} + 2.4326$$
 (2)

Where, T^* = temperature at tool pin periphery, T_{solidus} = solidus temperature of AA 2014-T6 aluminium alloy.

Table 1 Ratio of maximum temperature at tool pin periphery to the solidus temperature and the effective energy level using different tool pin profile of AA 2014-T6 aluminium alloy

Tool pin profile	T* (K)				Avg. T* (K)	T*/T _{solidus}	Q _{Eff/length}
	Trial 1	Trial 2	Trial 3	Trial 4	Avg. 1 (K)	1 / 1 solidus	♥Eff/length
TR	615	624	619	622	620	0.79	1162.25
SQ	612	623	619	618	618	0.79	1209.90
PEN	628	613	620	623	621	0.80	1257.56
HEX	631	623	625	629	627	0.80	1305.21

The modified generalized expression for total heat generation [7] in FSW process using different tool pin profiles considering mechanical efficiency (η) and heat generation due to plastic deformation (ϕ) is shown in Eqn. (3).

$$Q_{\text{Total}} = \frac{2}{3} \cdot \eta \cdot \varphi \cdot \pi \cdot \omega \cdot \mu \cdot \tau_{\text{contact}} \cdot \left(R^3 \text{shoulder} + X \cdot R^2 \text{probe} \cdot H_{\text{probe}} \right)$$
(3)

And the energy per unit length of the weld is shown in Eqn. (4)

$$Q_{\text{Energy/length}} = \frac{2}{3} \cdot \frac{\eta \cdot \varphi \cdot \omega \cdot \mu \cdot F}{\upsilon \cdot R^2 \text{shoulder}} \cdot \left(R^3 \text{shoulder} + X \cdot R^2 \text{probe} \cdot H_{\text{probe}} \right)$$
(4)

Where, ω is TRS, μ is friction coefficient, τ contact is contact shear stress, $R_{Shoulder}$ shoulder radius, R_{Probe} is pin radius, H_{Probe} is pin length, F is vertical force = 5 kN, υ is WS, η is mechanical efficiency, φ is heat generation due to plastic deformation which is 4.4% of the total heat generation for the FSW process [8] and the value of 'X' for TR, SQ, PEN and HEX tool pin profiles are 0.72, 0.95, 1.19, 1.43. The value of multiplying factor 'X' for straight cylindrical tool pin profile is 3 which indicates that maximum heat generated using straight cylindrical tool pin profile [7].

The sub-grain size at WZ obtained through pulsating stirring action is the function of strain rate and temperature. The effect of temperature and strain rate on the flow stress is well explained by the Zener–Hollomon parameter (Z) [9]:

$$Z = \varepsilon \times \exp^{\left(\frac{Q}{R \cdot T^*}\right)}$$
 (5)

Where ε is the strain rate (s-1), Q = 144 kJ/mol, is activation energy for process, R = 8.3145 J/mol/K [10], is universal gas constant, T^* is maximum temperature in K at tool pin periphery. ε is given as: $\varepsilon = \varepsilon/t$ where, ε is total strain at tool pin periphery, and t is time required for deformation and is calculated as: t = APR/v.

The estimation of total strain given by Reynolds [11] as:

$$\varepsilon = \ln\left(\frac{1}{APR}\right) + \left|\ln\left(\frac{APR}{1}\right)\right| \tag{6}$$

Where, APR is the tool advance per revolution (v/ω) and the method to calculate value of 'l' is given by Reynolds [11] as, a length of material equal to the APR in a streamline entering the pin-rounding flow field at the advancing edge is stretched to a length equal to the entire pin circumference. In the present case, for maximum strain value, the value of "l" is the perimeter of different tool pin profiles.

Finally, sub-grain size (d) is a function of Z parameter and can be estimated as:

$$d^{-1} = a + b \cdot \log(Z)$$
Where, $a = -1.095$, $b = 0.087$ are constitutive constants [10].

4. Results and discussion

4.1. Effect of different tool pin profiles on mechanical properties

The mechanical properties of the FSWed joints fabricated using different tool pin profiles are shown in Table 2. The transverse tensile properties such as yield strength (YS), ultimate tensile strength (UTS), percentage elongation (El), impact toughness and joint efficiency (η_{joint}) have been evaluated. At each condition, specimens were tested and average of the result is presented in Table 2. The weld specimen shows lower reduced strength and ductility due to the over-aged microstructure in heat affected zone (HAZ). The main reason to this observation could be the coarsened precipitates (CuAl₂) in HAZ [11-12].

		1 1		F -F	
	YS (N/mm2)*	UTS (N/mm2)*	El., (%)*	Impact Toughness (J)**	ηjoint(%)*
TR	202	267	2.7	4.67	48.79
SQ	215	323	3.4	5.33	51.93
PEN	207	260	2.5	3.67	50.00
HEX	193	249	2.1	3.33	46.62

Table 2 Effect of different tool pin profiles on mechanical properties of friction stir welds

^{*}Avg. of two and **Avg. of three

4.2. Effect of different tool pin profiles on microstructure

The grain size varies significantly with different tool pin profiles. The estimated average grain size is $1.135 \, \mu m$, $0.475 \, \mu m$, $0.74 \, \mu m$ and $0.765 \, \mu m$ for the TR, SQ, PEN and HEX tool pin profiles respectively using FEG-SEM. Heat and time (cooling and holding) play significant role in microstructural modification specifically longer holding time (explained in section 4.3) allows increase of grain size and significant densification of the material hence, modifying the properties and performance of the material.

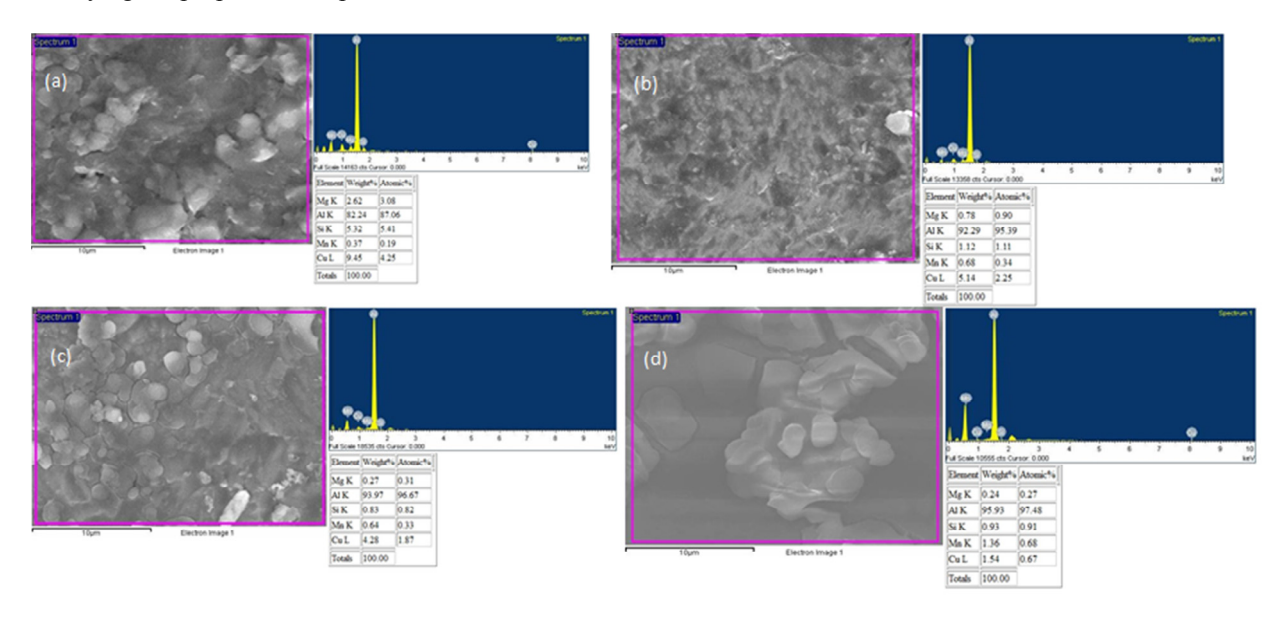


Fig. 4 FEG-SEM secondary electron image of the WZ of FSWment and EDS spectrum of a second-phase particles in the WZ using (a) TR, (b) SQ, (c) PEN, and (d) HEX tool pin profile.

Figure 4 shows FEG-SEM secondary electron image of the WZ of FSWeldment using TR to HEX tool pin profile and EDS spectrum of a second-phase particles in the weld region on EDS analysis. As shown in Fig. 4 (a), the EDS results demonstrate that using TR tool pin profile the particles in WZ contain higher concentrations of Al and Cu than the surrounding material. The EDS results from Fig. 4 (b-d) shows that using SQ to HEX tool pin profiles the particles in WZ contain reduction in concentrations of Cu, Mg, Si whereas increase concentration of Al, Mn in comparison with TR tool pin profile at WZ. Based on EDS analysis (Fig. 4 (a-d)), these particles were confirmed to be Al_2Cu (θ). Furthermore, it is known that alloy 2014 in T6 condition contains strengthening precipitates of λ ' ($Al_5Cu_2Mg_8Si_5$) and θ ' (Al_2Cu) phases. These observations corroborates with the findings of earlier studies on FSW of Al-Cu alloys [4, 12-14].

4.3. Effect of different tool pin profiles on thermal history

The peak temperature and cooling rate, experienced at any specific location in the joint during welding, are the key parameters which determine the microstructure and mechanical properties of welded joint [15]. The time to attain peak temperature is less in case of SQ tool pin profile whereas it is more in case of TR tool pin profile which is attributed due to less number of pulses and more time is required in case of TR tool pin profile for movement of one edge to get placed to another position of leading edge than SQ tool pin profile, causing solidification of material. The time duration for the material to experience temperatures over 200°C in TR tool pin profile welds is 15.87% longer than SQ tool pin profile welds. It is seen that TR tool pin profile welds give rise to higher temperature gradients due to more time to conduct the heat to the surroundings than SQ tool pin profile. This is also attributed to the relatively slower heat generation from Table 3.

	Table 3 Heating an	d cooling time	e using different too	pin profiles at	different temperatures
--	--------------------	----------------	-----------------------	-----------------	------------------------

	Time to reach (n	Time to reach (min.)							
Tool pin profile	Heating time		Cooling time						
	up to 200°C	up to 300°C	above 300°C to peak temperature	300°C-200°C					
TR	1.56	2.13	2.25	3.33					
SQ	1.37	1.52	2.20	3.25					
PEN	1.44	2.16	2.21	3.21					
HEX	1.49	2.13	2.23	3.43					

4.4. Process Map

The process map for different work material gives clear understanding of temperature, strain rate, plastic deformation, etc. behavior which will be helpful to optimize the FSW tool geometry and process parameters to get defect-free welds. According to process map which was developed for AA2024 aluminium alloy which is similar to AA2014 aluminium alloy, the dynamic recovery occurs in the temperature range of 340–420°C and at strain rates of 3–100/sec [16]. The temperature range (which is obtained using isothermal contour plot), analytically estimated strain-rate and Z parameter in the WZ from Eqn. (5) with the help of SQ tool pin profile are shown in Table 4. From the microstructure (Fig. 4b) of FSWs produced using SQ tool pin profile, fine grain structure was seen which is attributed due to 'Z' parameter at WZ (9.81×10¹¹) which falls in the dynamic recrystallization (9.26×10¹¹) region.

Table 4 Hot working ranges of temperature according to processing map [16] and estimated range of Z parameter using SQ tool pin profile

Condition	Temperature, °C (K)	Strain rate, s ⁻¹	Z parameter, s ⁻¹	Log (Z)
Di	380 (653)	0.001	5.68×10 ¹³	13.75
Dynamic recrystallization	500 (773)	10	9.26×10^{11}	11.97
Di	340 (613)	3	3.21×10^{14}	14.51
Dynamic recovery	420 (693)	100	1.23×10^{13}	13.09
Flow instability	< 330 (603)	>1	5.13×10 ¹⁴	14.71
WZ	498 (771)	172.26	9.81×10 ¹¹	11.99

Table 5 Estimated range of Z parameter using TR, PEN and HEX tool pin profiles with WZ temperature and strain rates

Condition	TR		PEN		HEX	
Condition	Z parameter, s ⁻¹	Log (Z)	Z parameter, s ⁻¹	Log (Z)	Z parameter, s ⁻¹	Log (Z)
Dymamia recorrectallization	5.60×10 ¹³	13.75	5.72×10 ¹³	13.76	5.74×10 ¹³	13.76
Dynamic recrystallization	9.12×10^{11}	11.96	9.32×10^{11}	11.97	9.35×10^{11}	11.97
Dynamic recovery	3.16×10 ¹⁴	14.50	3.23×10 ¹⁴	14.51	3.24×10 ¹⁴	14.51
	1.21×10^{13}	13.08	1.24×10^{13}	13.09	1.24×10^{13}	13.09
Flow instability	5.05×10 ¹⁴	14.70	5.16×10 ¹⁴	14.71	5.18×10 ¹⁴	14.71
	8.37×10 ¹¹	11.92	7.84×10 ¹¹	11.89	6.11×10 ¹¹	11.79
WZ	Temp., °C (K)	Strain rate	Temp., °C (K)	Strain rate	Temp., °C (K)	Strain rate
	503 (776)	169.71	506 (779)	173.41	515 (788)	174.03

The estimated range of Z parameter and strain-rate [16] using TR, PEN and HEX tool pin profiles are shown in Table 5. This indicates that 'Z' parameter at WZ falls in the dynamic recrystallization region using all tool pin profiles.

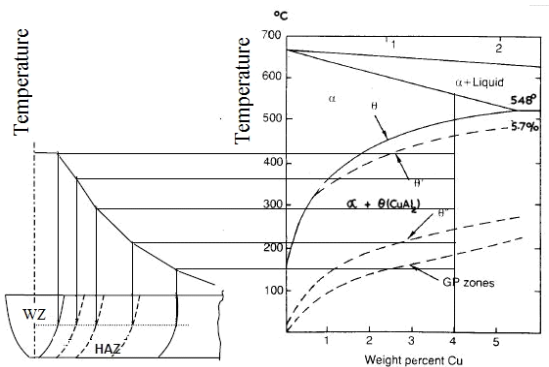


Fig. 5 The microstructures of the WZ and HAZ regions rationalized in terms of the Al-Cu phase diagram

Figure 5 shows the approximate correlation of microstructures of the WZ and HAZ regions in terms of the Al-Cu phase diagram. Figure 6 shows temperature contour plot and its correlation to microstructure for different tool pin profiles. Figure 6 shows the numerical results obtained from Comsol Multiphysics software [7]. Similar kinds of temperature trend were seen from analytical modelling (Table 1) and Numerical modelling (Fig. 6). From Fig. 6 (a) it is seen that the actual measured temperature for TR tool pin profile at 4 mm from joint line was closely resembles the recorded value.

It is seen that maximum temperature produced by HEX tool pin profile at WZ is closer to and above solidus temperature range. By correlating Fig. 5 with Fig. 6, it is seen that the peak temperatures at WZ produced by all pin profiles are in θ (Al₂Cu) and θ ' curve where all copper will be in solid solution as a stable fcc α phase. The transition phases θ " (discs) and θ ' (plates) are less stable than the equilibrium θ phase and consequently have higher free energies, whereas reversion takes place if temperature above the GP (Guinier-Preston) zone solvus, the zones will dissolve [17].

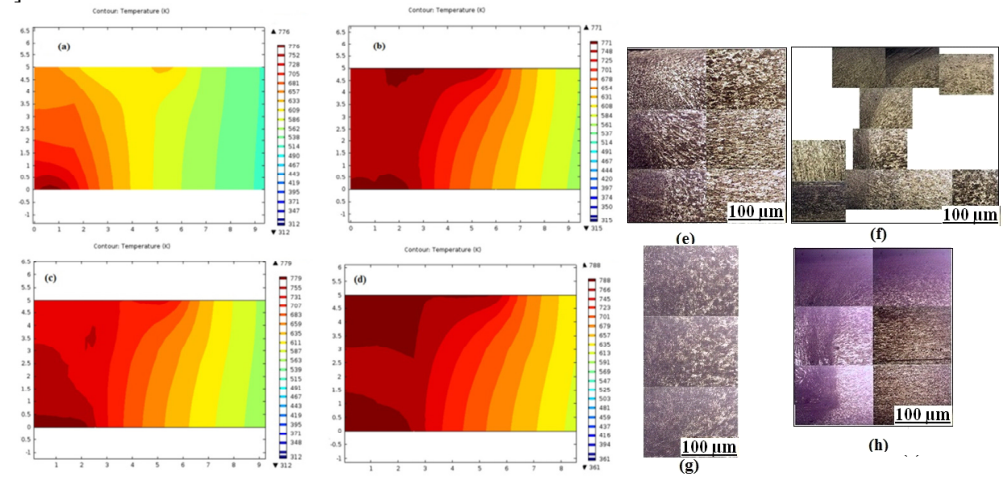


Fig. 6 Isothermal contour plot and its correlation to microstructure for (a, e) TR tool pin profile, (b, f) SQ tool pin profile, (c, g) PEN tool pin profile, and (d, h) HEX tool pin profile.

4.5. Effect of different tool pin profiles on strain rate and Z parameter

The effect of different tool pin profiles on analytically estimated values of total heat generation, effective energy per unit length, strain, strain rate, and Z parameter are shown in Table 6. The maximum temperature at WZ estimated using finite difference method, decreases from TR to SQ tool pin profile and again increases to HEX tool pin profile. The strain increases marginally as number of flats increases. Even though, ratio of dynamic to static volume is low for SQ compared to TR tool pin profile, it is offset by more number of pulses with better mechanical properties under given TRS.

Pin profile	T _{max} (K)	Q _{Total}	$Q_{\rm Eff/length}$	Strain	Strain rate (s ⁻¹)	Z	Log Z		ng layer ess, (μm)
	(14)							Expt.	drawing
TR	657	1009.76	1162.25	11.31	169.71	4.77×1013	13.68	69	150
SQ	654	1051.16	1209.90	11.48	172.26	5.46×1013	13.74	35	88
PEN	658	1092.56	1257.56	11.56	173.41	4.68×1013	13.67	32	57
HEX	667	1133.96	1305.21	11.60	174.03	3.29×1013	13.52	25	40

Table 6 Effect of different tool pin profiles on strain, strain rate, Z parameter and Rotating layer thickness

4.6. Effect of different tool pin profiles on rotating layer thickness

The shape of the WZ and HAZ region is a function of material, WS, and tool pin profile and can be obtained from the isotherms predicted by the solutions obtained from analytical equations [18]. The rotating layer refers to the annular mass of plasticized workpiece material that is driven around the tool pin [15]. Figure 7 (a) shows different pin geometries showing active surfaces responsible for deformation. The hatched region of respective tool pin profile indicates that these active surfaces are mainly responsible for shear deformation where sticking condition occurs, whereas sliding condition takes place over flat faces. Figure 7 (b) shows the typical shear deformation zone of TR, SQ, PEN and HEX tool pin profile stir welds. It is observed that the plasticized RLT adjacent to the tool pin profile is not uniform throughout the sheet thickness. The thickness of rotating layer is relatively more at the top of the cross section as compared to that at the bottom and is a function of tool pin profiles.

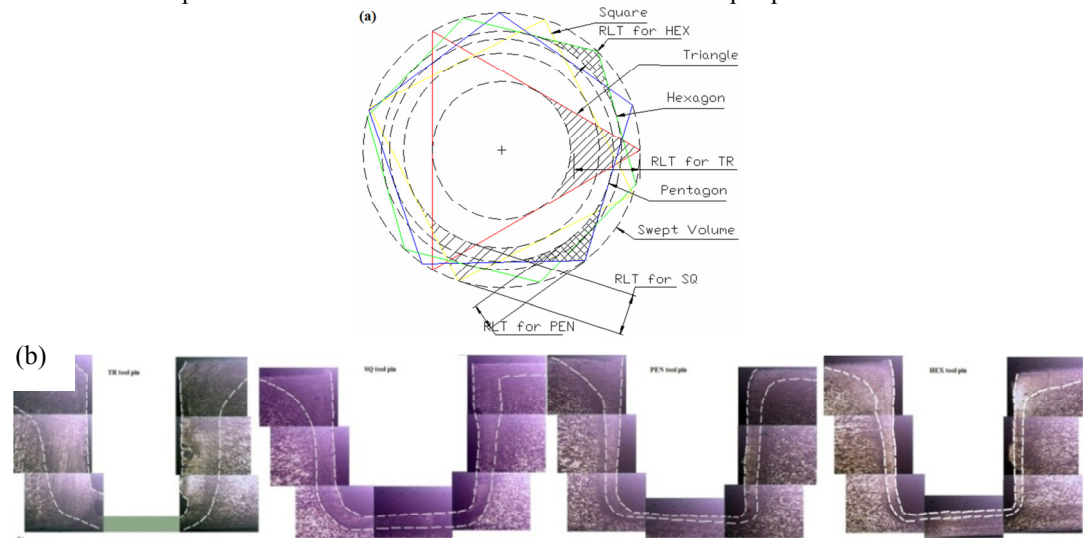


Fig.7 (a) Different pin profiles showing active surfaces responsible for deformation (b) variation of the active surfaces using different tool pin profiles.

Figure 7 (a-b) shows correlation of hatched region for respective tool pin profile with RLT. From Table 6 and Fig. 7 (a), it is seen that less surface area and more hatch region in case of TR tool pin profile corresponds to large value of RLT. Size of the deformation region (RLT) in the welds reduces with changing tool pin profile from TR to HEX tool pin profile.

5. Conclusions

In this work, the correlation of analytical modeling and microstructure of FSWed joints of AA 2014-T6 aluminium alloy produced using different tool pin profiles was done and following conclusions were drawn:

- Using developed analytical modeling, the effective energy per unit length of weld and strain rate increases from TR to HEX tool pin profiles.
- The peak temperatures measured at the WZ/TMAZ interface, below the shoulder, the peak temperature trend is monotonous using different tool pin profiles. Lowest peak temperature is observed for SQ tool pin profile whereas highest peak temperature is observed for HEX tool profile.
- From the analytical modeling, the value of Zener-Holloman parameter increases from TR to SQ then decreases to HEX tool pin profiles.
- Analytically estimated Zener-Holloman parameter value almost corroborates with estimated Zener-Holloman parameter value obtained from process map.
- Temperature contours for different tool pin profiles shows temperature flow pattern at different regions which shows a good co-relation with Al-Cu phase diagram.
- Experimentally, smallest grain size is observed for SQ tool pin profile which is attributed due to less temperature gradient compared to TR tool pin profile, more peak temperature rise and width of the peak producing annealing effect which may cause for better mechanical property.

Acknowledgements

The authors would like to thank the authorities of NIT, Warangal, India. Also, authors would like to thank Prof. Indradev Samajdar, Head, SAIF, IIT Bombay for providing FEG-SEM facility for SEM and EDS analysis. One of the authors (V. S. Gadakh) gratefully acknowledges the support of the SPPU, Pune Grant # 13ENG000074.

References

- [1] ASM Handbook-Vol. 2 Properties and selection: Nonferrous alloys and special-purpose materials. ASM International, 1992.
- [2] N. Rajamanickam, V. Balusamy, G. M. Reddy, K. Natarajan, Mater. Des., 30 (2009) 2726–2731.
- [3] W. M. Thomas, Friction stir butt welding, International Patent Application PCT/GB92/02203 and GB Patent Application 9125978-8, 1991.
- [4] R. S. Mishra and Z. Y. Ma, 50 (2005) 1–78.
- [5] M.K.B. Givi, P. Asadi, Advances in Friction Stir Welding and Processing. Woodhead Publishing, 2014.
- [6] C. Hamilton, S. Dymek, A. Sommers, Int. J. Mach. Tools Manuf. 48 (2008) 1120–1130.
- [7] V. S. Gadakh, A. Kumar, G. J. Vikhe Patil, Weld. J. 93 (2015) 115s–124s.
- [8] A. R. Darvazi, M. Iranmanesh, Mater. Des. 55 (2014) 812–820.
- [9] F. J. Humphreys, M. Hatherly, Recrystallization and related annealing phenomena, 2nd Ed. Elsevier, 2004.
- [10] A. Gerlich, P. Su, M. Yamamoto, T. H. North, J. Mater. Sci. 42 (2007) 5589-5601.
- [11] A. P. Reynolds, Scr. Mater. 58 (2008) 338-342.
- [12] M. Mahoney, C. Rhodes, J. Flintoff, W. Bingel, R. Spurling, Metall. Mater. Trans. A 29 (1998) 1955–1964.
- [13] R. Nandan, T. Debroy, H. K. D. H. Bhadeshia, Prog. Mater. Sci. 53 (2008) 980-1023.
- [14] G. M. Reddy, P. Mastanaiah, K. S. Prasad, T. Mohandas, Trans. Indian Inst. Met. 62 (2009) 49-58.
- [15] K. Ramanjaneyulu, G. M. Reddy, A. V. Rao, R. Markandeya, J. Mater. Eng. Perform. 22 (2013) 2224-2240.
- [16] Y.V.R.K. Prasad, S. Sasidhara, Hot Working Guide: A Compendium of Processing Maps, ASM International, 1997, pp. 50-52.
- [17] D. A. Porter, K. E. Easterling, Phase transformations in metals and alloys, 2nd ed. Chapman & Hall, 1996.
- [18] R. W. J. Messler, Principles of welding-Processes, Physics, Chemistry, and Metallurgy. Wiley-VCH Verlag GmbH & Co. Weinheim, 2004.